J. Fluid Mech. (1973), *vol.* 58, *part* 4, *pp.* 795–815
Printed in Great Britain

The interaction of a transient exhaust plume with a rarefied atmosphere

By HOWARD R. BAUM
Aerodyne Research, Inc., Burlington, Mass. 01803, U.S.A.

(Received 5 October 1972 and in revised form 23 February 1973)

The interaction of a gas cloud of specified mass, momentum and energy with an atmosphere in uniform motion is studied using the kinetic theory of gases. The Krook collision model is used to obtain analytically interpretable and numerically tractable results describing the spatial and temporal evolution of the cloud. The cloud originates from a continuum source and expands to a free molecular flow. It then begins to collide with the atmosphere, and is gradually transformed into a continuum flow diffusing through the atmosphere while being convected by the uniform motion.

1. Introduction

The rarefaction of a continuum gas jet as it expands into a near vacuum has been extensively studied in recent years. These studies have application to rocket exhaust plumes and molecular beams. They are also extremely interesting in their own right as a problem in gasdynamics in which the flow regime changes from continuum to free molecular and back again.

Consider the flow pattern set up by a nozzle emitting an exhaust gas for a finite duration and then shutting down. The Knudsen number at the nozzle exit in the steady state is assumed to be sufficiently small for a region of continuum flow to exist. The flow near the exhaust plume centre-line may be studied by considering a spherically symmetric source expanding into a vacuum. The steady source problem (in both spherical and cylindrical geometry) has been investigated by Brook & Oman (1965), Edwards & Cheng (1966), Hamel & Willis (1966), Chen (1970) and Thomas (1971). The corresponding unsteady expansions have been analysed by Freeman & Grundy (1968) and Grundy & Thomas (1969). Some properties of an axially symmetric expansion have been considered by Grundy (1969); while Peracchio (1970) has studied the flow pattern created by a two-dimensional nozzle. The above studies follow the rarefaction through the onset of translational non-equilibrium into a free molecular flow. A useful estimate of the point at which translational 'freezing' occurs in rocket exhaust plumes is given by Draper & Hill (1969). When the background density is sufficiently low for the ambient mean free path to be much larger than the distance from the nozzle exit to the region where translational non-equilibrium occurs, the interaction of the exhaust gas with the atmosphere is decoupled from the initial rarefaction process. This fact has been exploited by

Brook & Hamel (1972) in their analysis of the expansion of a spherical source into a stationary background gas.

The present work considers the time-dependent interaction of a finite gas cloud formed by the pulsed operation of a rocket motor with a low-density background in uniform motion. The number, momentum and energy of the exhaust gas molecules are assumed to be small compared with those of the background molecules contained in a cube of side one mean free path. The initial rarefaction region is represented by a transient point source with this prescribed flux of mass, momentum and energy. The interaction of the exhaust gas with the background gas then becomes a linear problem. The Krook collision integral is used to represent the collision dynamics and permits the construction of analytical solutions.

This calculation is applicable to an attitude control or other small motor operating at very high altitudes. Such motors often have a firing time which is comparable with or even less than the mean time between collisions at the operating altitude. Since the natural time scale for the interaction is the mean time between collisions, this process is essentially unsteady, even if the flow near the nozzle exit is steady while the rocket is firing.

The solution has the form of a bimodal distribution function. For times smaller than the ambient mean collision time the gas is essentially in free molecular flow, and the distribution function is determined by the properties of the steady rarefaction that existed near the nozzle exit while the motor was operating. This free molecular solution is multiplied by an exponentially decaying function of time, representing the decay of the beam by collisions with the atmosphere. The details of the collision process are represented by the second term in the distribution function. This term has the form of the convolution over space and time of the free molecular flow with a scattering Green's function. The scattering function contains the ambient atmosphere parameters, while the free molecular function contains the rocket engine parameters. In addition, although the overall flow is three-dimensional and unsteady, none of the separate components of the solution each contain all possible independent variables. The free molecular flow is axially symmetric, the axis of symmetry being the rocket thrust axis. The scattering function depends on the time measured in units of reciprocal ambient collision frequency. The scalar distance variable is measured from a point $\mathbf{u}_\infty t$ removed from the rocket engine where $\mathbf{u}_\infty$ is the ambient wind velocity in the engine rest frame. The distance is measured in ambient mean free path units. After several collision times, the scattering function becomes the macroscopic diffusion Green's function, and the expansion process ultimately is describable as macroscopic diffusion in a uniformly moving stream.

2. Mathematical formulation

The motion of the exhaust molecules is described by a distribution function $f(\mathbf{x}, \mathbf{v}, t)$, the phase space density. The distribution is assumed to satisfy the kinetic equation

$$\frac{\partial f}{\partial t} + \mathbf{v}.\frac{\partial f}{\partial \mathbf{x}} = \omega(n\Phi - f) + \omega_a(n\Phi_a - f) + \delta(\mathbf{x})\, Q_0(t)\, \Phi_s(\mathbf{v}). \tag{1}$$

Here $\delta(\mathbf{x})$ is a delta function located at the nozzle exit $\mathbf{x} = 0$ and

$$\Phi = \left(\frac{m}{2\pi kT}\right)^{\frac{3}{2}} \exp\left[-\frac{m}{2kT}(\mathbf{v}-\mathbf{u})^2\right] \equiv \Phi(\mathbf{u}, T),$$
$$\Phi_s = \Phi(\mathbf{u}_s, T_s), \quad \Phi_a = \Phi(\mathbf{u}_a, T_a).$$

The number density n, macroscopic velocity $\mathbf{u}$ and temperature T of the exhaust gas are defined as moments of the distribution function:

$$n(\mathbf{x}, t) = \int f d^3v, \quad n\mathbf{u}(\mathbf{x}, t) = \int \mathbf{v} f d^3v, \tag{2a, b}$$

$$\tfrac{3}{2}nkT(\mathbf{x}, t) = \int \tfrac{1}{2}m(\mathbf{v}-\mathbf{u})^2 f d^3v. \tag{2c}$$

The first term on the right-hand side of (1) represents the interaction of the exhaust gas with itself. The self-collision frequency ω is proportional to the density. This makes the term first dominant near the nozzle exit and negligible far from it. Since the interaction of the exhaust with theambient background is the subject of the investigation, this term will be carried along solely to estimate the residual effect of self-collisions on the far field. The second term on the right-hand side of (1) describes the interaction of the exhaust with the background atmosphere. The ambient velocity $\mathbf{u}_a$ and temperature T_a are constant because the exhaust gas is so dilute by the time it interacts with the atmosphere that only small changes in ambient macroscopic properties can occur. This interaction term differs from that given by Gross & Krook (1956). Conservation of momentum and energy requires that $\mathbf{u}_a$ and T_a be replaced by their respective effective interaction quantities $\mathbf{u}_{ea}$ and T_{ea}. For example, conservation of momentum leads to the well-known expression

$$\mathbf{u}_{ea} = (m\mathbf{u} + m_a\mathbf{u}_a)/(m+m_a).$$

However, the momentum of the exhaust gas is *not* conserved. The rate at which momentum is transferred to the exhaust gas is given by (1) as

$$\omega_a nm(\mathbf{u}_a - \mathbf{u}).$$

By using the above expression for $\mathbf{u}_{ea}$, the momentum transfer rate is found to be

$$\omega_a n \frac{mm_a}{m+m_a}(\mathbf{u}_a - \mathbf{u}),$$

where $\mathbf{u}$ is the velocity defined in (2b). Thus, by writing $\omega_a = m_a/(m+m_a)\overline{\omega}_a$, the two expressions can be made identical for any choice of collision frequency ω_a. Similar remarks apply to the energy transfer. Since attention may be confined to the exhaust gas (the background gas being a uniform source or sink of momentum and energy), the only conserved quantity of interest is the number (or mass) of exhaust molecules. This quantity is conserved in the present formulation.

The final term (1) is the source of the exhaust gas that is used to represent continuum flow near the nozzle exit. The point-source representation is justified when the dimensions of the translational freezing surface (see Draper & Hill 1969) are much smaller than the mean free path for the interaction of the exhaust gas with the atmosphere. The parameters $Q_0(t)$, $\mathbf{u}_s$ and T_s are determined by equating the mass, momentum and energy flux of the source to the corresponding properties of the nozzle exit. Thus

$$mQ_0 = (\rho u A)_e, \quad mQ_0 \mathbf{u}_s = [(p+\rho u^2) A]_e \, \mathbf{s}, \tag{3a,b}$$

$$[(h+\tfrac{1}{2}u^2)\rho u A]_e = Q_0 [\tfrac{1}{2}mu_s^2 + \tfrac{3}{2}kT_s + \epsilon(T_s)]. \tag{3c}$$

The subscript e in (3) refers to nozzle exit conditions averaged over the nozzle exit area A. The quantities p, ρ and h are the pressure, density and enthalpy of the gas, while $\mathbf{s}$ is a unit vector in the direction of the thrust. The internal energy per molecule at the exit is $\frac{3}{2}kT + \epsilon(T)$, where $\epsilon(T)$ is the average energy per molecule frozen in internal (non-translational) degrees of freedom. $\epsilon(T)$ can be evaluated in terms of the specific heat ratio γ at the exit. Let the average number of excited degrees of freedom be α (not necessarily an integer). Then

$$\tfrac{3}{2}kT_s + \epsilon(T_s) = \alpha k T_s, \tag{4}$$
$$\gamma = C_p/C_v = (1+\alpha)/\alpha.$$

Equations (3) and (4) can be manipulated to yield the expressions

$$u_s = u_e\left[\frac{1}{\gamma M_e^2} + 1\right] \tag{5a}$$

$$W_s^2 \equiv \frac{u_s^2}{2kT_s/m} = \frac{(1+\gamma M_e^2)^2}{2\gamma M_e^2 - (\gamma-1)}, \tag{5b}$$

$$\frac{T_s}{T_e} = \frac{1}{2}\frac{2\gamma M_e^2 - (\gamma-1)}{1+\gamma M_e^2}. \tag{5c}$$

The source properties evidently become the exit properties as the exit Mach number M_e becomes large. It should be noted that the exit Mach numbers M_e implied in this calculation are supersonic and the apparent singularity in (5b) at $M_e^2 = (\gamma-1)/2\gamma$ cannot occur.

The parameter $Q_0(t)$ is the total particle flux emitted by the nozzle. The nozzle is assumed to operate with uniform conditions for a time t_0 and then shut down instantaneously. Thus

$$Q_0(t) = \begin{cases} Q_0, & 0 < t < t_0, \\ 0, & t > t_0. \end{cases} \tag{6}$$

The mathematical model of the exhaust gas interaction then consists of (1) and (2), which hold for all $\mathbf{x}$ and all $t > 0$. The continuum region near the nozzle is represented by a point source at $\mathbf{x} = 0$ whose parameters are defined by (3)–(6). Initially there are no exhaust particles:

$$f(\mathbf{x}, \mathbf{v}, t) = 0 \quad \text{at} \quad t = 0. \tag{7}$$

The formulation is consistent if $Q_0 t_0/n_a\lambda_a^3 \ll 1$, where λ_a is mean free path for collisions with ambient molecules and n_a is the ambient density. λ_a is related to the ambient collision frequency ω_a by

$$\omega_a \lambda_a = (2kT_a/m)^{\frac{1}{2}}.$$

This inequality is the mathematical statement of the condition that the exhaust gas concentration n/n_a is small on the scale on which the interaction occurs.

3. Formal solution

The formal solution to (1) is obtained by transform methods. Define the Fourier–Laplace transform of any function $g(\mathbf{x}, t)$ as follows:

$$\bar{g}(\mathbf{k}, p) \equiv \int d^3x \int_0^\infty dt\, e^{-i\mathbf{k}.\mathbf{x}-pt} g(\mathbf{x}, t), \tag{8a}$$

$$g(\mathbf{x}, t) = \int \frac{d^3k}{(2\pi)^3} \int_C \frac{dp}{2\pi i} e^{pt+i\mathbf{k}.\mathbf{x}} \bar{g}(\mathbf{k}, p). \tag{8b}$$

Now multiply (1) by $e^{-i\mathbf{k}.\mathbf{x}-pt}$, integrate over all $\mathbf{x}$ and all $t > 0$, and use (7) and (8) to get

$$(p + i\mathbf{k}.\mathbf{v} + \omega_a)\bar{f} - \omega_a \Phi_a \bar{n} = \omega\overline{(n\Phi - f)} + \bar{Q}_0(p)\,\Phi_s. \tag{9}$$

Using (2*a*) and (9) the transformed number density is found to be

$$\bar{n} = \left\{1 - \omega_a \int \frac{\Phi_a(\mathbf{v})\, d^3v}{p + i\mathbf{k}.\mathbf{v} + \omega_a}\right\}^{-1} \left\{\int \frac{\overline{\omega(n\Phi - f)}}{p + i\mathbf{k}.\mathbf{v} + \omega_a} d^3v + \bar{Q}(p) \int \frac{\Phi_s(\mathbf{v})\, d^3v}{p + i\mathbf{k}.\mathbf{v} + \omega_a}\right\}. \tag{10}$$

In order to proceed further, it is necessary to consider the solution (10) as a function of p for fixed real $\mathbf{k}$. The two expressions in the second curly bracket each converge separately for large p. They represent Laplace transforms of physically acceptable functions which will be studied in detail below. The first curly bracket however, is not convergent as it stands. Thus, in order to apply the convolution theorem to (10), the first factor must be rewritten as

$$1 + \omega_a \int \frac{\Phi_a(\mathbf{v})\, d^3v}{p + i\mathbf{k}.\mathbf{v} + \omega_a} \left[1 - \omega_a \int \frac{\Phi_a(\mathbf{v})\, d^3v}{p + i\mathbf{k}.\mathbf{v} + \omega_a}\right]^{-1}.$$

The solution may now be written as

$$\bar{n}(\mathbf{k}, p) = \bar{n}_1(\mathbf{k}, p) + \bar{n}_2(\mathbf{k}, p) + \bar{n}_3(\mathbf{k}, p), \tag{11a}$$

$$\bar{n}_1 = \bar{Q}(p) \int \frac{\Phi_s(\mathbf{v})\, d^3v}{p + i\mathbf{k}.\mathbf{v} + \omega_a}, \quad \bar{n}_2 = \int \frac{\overline{\omega(n\Phi - f)}\, d^3v}{p + i\mathbf{k}.\mathbf{v} + \omega_a}, \quad \bar{n}_3 = (\bar{n}_1 + \bar{n}_2)\, \bar{G}(p, \mathbf{k}), \tag{11b}$$

$$\bar{G}(p, \mathbf{k}) = \omega_a \int \frac{\Phi_a(\mathbf{v})\, d^3v}{p + i\mathbf{k}.\mathbf{v} + \omega_a} \left[1 - \omega_a \int \frac{\Phi_a(\mathbf{v})\, d^3v}{p + i\mathbf{k}.\mathbf{v} + \omega_a}\right]^{-1}. \tag{11c}$$

The first term $n_1(\mathbf{x}, t)$ is a free molecular flow originating at the source which is continuously depleted by collisions with the atmosphere. The term $n_2(\mathbf{x}, t)$ is the correction to this flow arising from the remaining self-interactions of exhaust molecules outside the continuum region. The third term $n_3(\mathbf{x}, t)$ represents the interaction of the free molecular flow $n_1 + n_2$ with the atmosphere. The interaction is represented by a convolution of $n_1 + n_2$ with an interaction Green's function $G(\mathbf{x}, t)$. These three expressions will now be studied in detail.

4. Source flow

The source flow $n_1(\mathbf{x}, t)$ may itself be represented as a convolution of the particle flux history $Q_0(t)$ with the inverse of the remaining expression in $\bar{n}_1(\mathbf{k}, p)$. Thus

$$n_1(\mathbf{x}, t) = \int_0^t dt'\, Q_0(t-t') \int d^3v\, \Phi_s(\mathbf{v}) \frac{1}{(2\pi)^3\, 2\pi i} \iint \frac{d^3k\, dp\, e^{i\mathbf{k}.\mathbf{x}+pt'}}{p+i\mathbf{k}.\mathbf{v}+\omega_a}. \tag{12}$$

The integrals over $\mathbf{k}$ and p can easily be carried out to yields

$$\frac{1}{2\pi i (2\pi)^3} \iint \frac{d^3k\, dp\, e^{i\mathbf{k}.\mathbf{x}+pt'}}{p+i\mathbf{k}.\mathbf{v}+\omega_a} = e^{-\omega_a t'}\, \delta(\mathbf{x}-\mathbf{v}t').$$

Substituting this result back into (12), integrating over $\mathbf{v}$ and using the expression (6) for $Q_0(t)$ gives

$$n_1(x, t) = \begin{cases} Q_0 \displaystyle\int_{t-t_0}^t dt' \frac{e^{-\omega_a t'}}{t'^3}\, \Phi_s\!\left(\frac{\mathbf{x}}{t'}\right) & (t > t_0), \\ Q_0 \displaystyle\int_0^t dt' \frac{e^{-\omega_a t'}}{t'^3}\, \Phi_s\!\left(\frac{\mathbf{x}}{t'}\right) & (0 < t < t_0). \end{cases} \tag{13}$$

At this point it is appropriate to define a coordinate system. The unit thrust vector $\mathbf{s}$ and the ambient velocity $\mathbf{u}_a$ define a plane. Define a unit vector $\mathbf{a}$ such that $\mathbf{u}_a = u_a \mathbf{a}$. Let ψ be the angle between $\mathbf{s}$ and $\mathbf{a}$. A right-handed Cartesian co-ordinate system is then (see figure 1)

$$\mathbf{i} = \frac{(\mathbf{s}\times\mathbf{a})\times\mathbf{s}}{\sin\psi}; \quad \mathbf{j} = \frac{\mathbf{s}\times\mathbf{a}}{\sin\psi}; \quad \mathbf{s}.$$

Spherical co-ordinates, with the polar angle θ measured from $\mathbf{s}$ and the azimuthal angle ϕ measured from $\mathbf{i}$ allow the position vector $\mathbf{x}$ and the velocity $\mathbf{u}_a$ to be represented as

$$\left.\begin{aligned} \mathbf{x} &= x\left\{\frac{(\mathbf{s}\times\mathbf{a})\times\mathbf{s}}{\sin\psi}\sin\theta\cos\phi + \frac{\mathbf{s}\times\mathbf{a}}{\sin\psi}\sin\theta\sin\phi + \mathbf{s}\cos\theta\right\}, \\ u_a &= u_a\left\{\frac{(\mathbf{s}\times\mathbf{a})\times\mathbf{s}}{\sin\psi}\sin\psi + \mathbf{s}\cos\psi\right\}. \end{aligned}\right\} \tag{14}$$

Returning to the solution (13) the integrals may be explicitly calculated for the important case $\omega_a t_0 \ll 1$. Under these conditions

$$\int_{t-t_0}^t dt' \frac{e^{-\omega_a t'}}{t'^3}\, \Phi_s\!\left(\frac{\mathbf{x}}{t'}\right) \cong e^{-\omega_a t} \int_{t-t_0}^t dt'\, t'^{-3}\, \Phi_s\!\left(\frac{\mathbf{x}}{t'}\right).$$

Using t'^{-1} as the variable of integration the above expression is easily evaluated, yielding

$$n_1(x, t) = \frac{Q_0 e^{-\omega_a t}}{\pi^{\frac{3}{2}} x^2} \left(\frac{m}{2kT_s}\right)^{\frac{1}{2}} \exp(-W_s^2 \sin^2\theta)\,[-F_1(\alpha)+F_1(\beta)], \tag{15a}$$

$$F_1(\beta) = \tfrac{1}{2}\pi^{\frac{1}{2}} W_s \cos\theta\, \mathrm{erf}\,\beta - \tfrac{1}{2} e^{-\beta^2}, \tag{15b}$$

$$\alpha = W_s\left(\frac{x}{u_s t} - \cos\theta\right), \quad \beta - \alpha = \frac{W_s x}{u\ t}\left(\frac{t_0}{t-t_0}\right). \tag{15c}$$

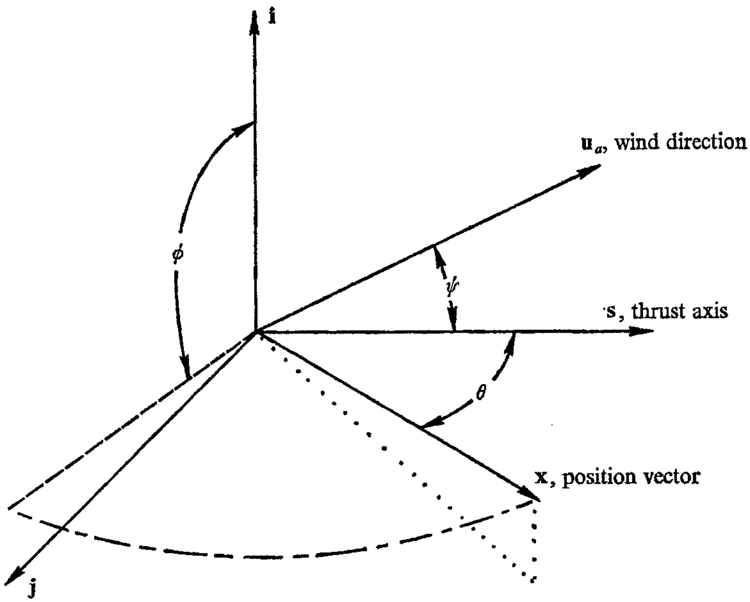

FIGURE 1. Co-ordinate system employed showing the wind axis **a**, the thrust axis **s** and the position vector **x**. Nozzle exit at the origin.

This result applies for times $t > t_0$. For times $t < t_0$, solution (15) applies with the value of β taken as $+\infty$. Thus

$$n_1(\mathbf{x}, t) = \frac{Q_0 e^{-\omega_a t}}{4\pi x^2} \frac{2m^{\frac{1}{2}}}{\pi k T_s} \exp\left(-W_s^2 \sin^2\theta\right) \{\pi^{\frac{1}{2}} W_s \cos\theta \operatorname{erfc}\alpha + e^{-\alpha^2}\}; \quad 0 < t < t_0. \tag{16}$$

Note that when the factor $\exp(-\omega_a t)$ is omitted (15) is an exact solution to the free molecular pulsed source, while (16) is the corresponding solution for the initiation of a steady source. These free molecular flows are of interest in their own right and will be briefly considered here. The distribution function $f_1(\mathbf{x}, \mathbf{v}, t)$ associated with n_1 is easily seen from (12) to be

$$f_1(\mathbf{x}, \mathbf{v}, t) = \int_{t-t_0}^{t} dt' \, e^{-\omega_a t'} Q_0 \delta(\mathbf{x} - \mathbf{v}t') \, \Phi_s(\mathbf{v}). \tag{17}$$

Multiplying (17) by $\mathbf{v}$, integrating over $\mathbf{v}$ and assuming $\omega_a t_0 \ll 1$ yields

$$n_1 \mathbf{u}_1(\mathbf{x}, t) = \frac{\mathbf{x}}{x} \frac{Q_0}{x^2} \frac{\exp\left(-\omega_a t - W_s^2 \sin^2\theta\right)}{\pi^{\frac{3}{2}}} [F_2(\beta) - F_2(\alpha)], \tag{18}$$

$$F_2(\alpha) = -\tfrac{1}{2}\pi^{\frac{1}{2}} \left(W_s^2 \cos^2\theta + \tfrac{1}{2}\right) \operatorname{erf}\alpha - \left(W_s \cos\theta + \tfrac{1}{2}\alpha\right) e^{-\alpha^2}.$$

Next multiply (17) by v^2 and carry out the same procedure to obtain

$$3\frac{nkT_1}{m} + nu_1^2 = Q_0 \left(\frac{2kT_s}{m}\right)^{\frac{1}{2}} \frac{\exp\left(-\omega_a t - W_s^2 \sin^2\theta\right)}{x^2 \pi^{\frac{3}{2}}} [F_3(\beta) - F_3(\alpha)], \tag{19}$$

$$F_3(\alpha) = \tfrac{1}{2}\pi^{\frac{1}{2}} W_s \cos\theta \left[\tfrac{3}{2} + (W_s \cos\theta)^2\right] \operatorname{erf}\alpha - \left\{\tfrac{1}{2}(\alpha^2 + 1) + \tfrac{3}{2} W_s \cos\theta (\alpha + W_s \cos\theta)\right\} e^{-\alpha^2}.$$

Finally, (17)–(19) may be combined to solve for $\mathbf{u}_1$ and T_1:

$$\mathbf{u}_1(\mathbf{x},t) = \frac{\mathbf{x}}{x}\left(\frac{2kT_s}{m}\right)^{\frac{1}{2}} \frac{F_2(\beta)-F_2(\alpha)}{F_1(\beta)-F_1(\alpha)}, \tag{20a}$$

$$T_1(\mathbf{x},t) = T_s \frac{2}{3}\frac{[F_3(\beta)-F_3(\alpha)]\,[F_1(\beta)-F_1(\alpha)]-[F_2(\beta)-F_2(\alpha)]^2}{[F_1(\beta)-F_1(\alpha)]^2}. \tag{20b}$$

Equations (15) and (20) constitute the free molecular solution to the pulsed source problem, while the starting flow is given by (16) and (20) with $\beta = \infty$.

These solutions illustrate the qualitative difference in the asymptotic behaviour of the kinetic temperature of a steady expansion as opposed to that of a pulsed flow. First consider the steady case. The temperature is obtained from (20b) by setting $\beta = \infty$ and $\alpha = -W_s \cos\theta$. Thus

$$F_3(\beta) = \tfrac{1}{2}\pi^{\frac{1}{2}} W_s \cos\theta\,[\tfrac{3}{2} + (W_s\cos\theta)^2],$$

$$F_2(\beta) = \tfrac{1}{2}\pi^{\frac{1}{2}}(W_s^2\cos^2\theta + \tfrac{1}{2}), \quad F_1(\beta) = \tfrac{1}{2}\pi^{\frac{1}{2}} W_s \cos\theta.$$

Since $F_1(\alpha)$, $F_2(\alpha)$ and $F_3(\alpha)$ are all bounded $T_1(\mathbf{x})$ depends only on θ. In particular there is no radial decay. Next consider the transient pulsed case. For values of $t_0/t \ll 1$, β approaches α. In fact

$$\beta - \alpha \cong \frac{W_s x}{u_s t}\frac{t_0}{t}.$$

Now expand the solutions in a Taylor series in $\beta-\alpha$ to get

$$\mathbf{u}_1(\mathbf{x},t) \cong \frac{\mathbf{x}}{x}\left(\frac{2kT_s}{m}\right)^{\frac{1}{2}} \frac{F_2'(\alpha)}{F_1'(\alpha)} = \frac{\mathbf{x}}{t}, \tag{21a}$$

$$T_1(\mathbf{x},t) \cong \frac{T_s}{18}(\beta-\alpha)^2 = \frac{m}{36k}\left(\frac{x}{t}\right)^2\left(\frac{t_0}{t}\right)^2, \tag{21b}$$

$$n_1(\mathbf{x},t) \cong \frac{Q_0 t_0}{\pi^{\frac{3}{2}} t^3}\left(\frac{W_s}{u_s}\right)^3 \exp\left[-W_s^2\sin^2\theta - W_s^2\left(\frac{x}{u_s t} - \cos\theta\right)^2 - \omega_a t\right]. \tag{21c}$$

Equation (21b) shows that in the expanding shell that constitutes the free molecular gas cloud the temperature is decreasing at a rate proportional to $(t_0/t)^2$. Moreover, the velocity is radial and the maximum density on each ray is located at $x = u_s t \cos\theta$.

The density is approximately spherically symmetric about the point

$$\mathbf{x} = \mathbf{u}_s t \quad \text{for} \quad t \gg t_0$$

and decreases in magnitude like $t^{-3}e^{-\omega_a t}$.

5. Self-scattering effects

The purpose of this section is to estimate the relative importance of the source and self-scattering contributions (n_1 and n_2 respectively in (11)) to the density. Since the source term is assumed to contain the continuum region dominated by self-collisions, it is reasonable to anticipate that it is the more important one. The approach used in this section is to assume that the formal solution $n_2(\mathbf{x},t)$

can be evaluated using the expressions obtained in the preceding section for the source flow $n_1(\mathbf{x},t)$. The result that n_2 is indeed much smaller than n_1 then provides the required check on the calculation.

The inversion of $\bar{n}_2(\mathbf{k},p)$ in (11*b*) may be performed with the aid of the convolution theorem to give

$$n_2(\mathbf{x},t) = \int d^3v \int_0^t dt' \int d^3y\, Z(\mathbf{y},\mathbf{v},t')\, \delta[\mathbf{x}-\mathbf{y}-\mathbf{v}(t-t')]\, e^{-\omega_a(t-t')}, \tag{22}$$

$$Z \equiv \omega(n\Phi - f) = Z(\mathbf{x},\mathbf{v},t).$$

Carrying out the $\mathbf{v}$ integration yields

$$n_2(\mathbf{x},t) = \int_0^t dt' \int d^3y \frac{e^{-\omega_a(t-t')}}{(t-t')^3} Z\left[y, \frac{(\mathbf{x}-\mathbf{y})}{t-t'}, t'\right]. \tag{23}$$

The role of $n_2(\mathbf{x},t)$ as a rearrangement of the source flow $n_1(\mathbf{x},t)$ can now be made clear. Integrating (23) over all $\mathbf{x}$ and using the mass conservation property of the self-collision term yields the result

$$\int n_2(\mathbf{x},t)\, d^3x = 0.$$

The distribution function $f_2(\mathbf{x},\mathbf{v},t)$ associated with n_2 also conserves momentum and energy. Inspection of (22) yields the expression for $f_2(\mathbf{x},\mathbf{v},t)$:

$$f_2(\mathbf{x},\mathbf{v},t) = \int_0^t dt' \int d^3y Z(\mathbf{y},\mathbf{v},t)\, \delta[\mathbf{x}-\mathbf{y}-\mathbf{v}(t-t')]\, e^{-\omega_a(t-t')}.$$

The properties of the collision integral Z then require that

$$\int d^3x \int m\mathbf{v} f_2\, d^3v = 0, \quad \int d^3x \int \tfrac{1}{2}mv^2 f_2\, d^3v = 0.$$

The total mass, momentum and energy emitted by the nozzle is thus contained in the source term. The self-collision term spatially redistributes the exhaust gas without affecting the conserved quantities. The magnitude of this redistribution that can occur outside the continuum region will now be estimated. The quantities entering into the self-collision term $Z(\mathbf{x},\mathbf{v},t)$ will be evaluated using the corresponding results from the source flow term in accordance with the scheme outlined at the beginning of this section.

First consider the loss term n_{2L} in (23) defined by

$$n_{2L} = -\int_0^t dt' \int d^3y \frac{e^{-\omega_a(t-t')}}{(t-t')^3} \omega f\left(\mathbf{y}, \frac{\mathbf{x}-y}{t-t'}, t'\right), \tag{24}$$

$$f = Q_0 e^{-\omega_a t} \int_{t-t_0}^{t} dt''\, \delta(\mathbf{x}-\mathbf{v}t'')\, \Phi_s(\mathbf{v}).$$

When the spatial integration is carried out, (24) reduces to

$$n_{2L} = -Q_0\, e^{-\omega_a t} \int_0^t dt' \int_{t'-t_0}^{t'} dt'' \left[\frac{1}{t-(t'-t'')}\right]^3 \omega\left(\frac{\mathbf{x}t''}{t-(t'-t'')}, t'\right) \Phi_s\left(\frac{\mathbf{x}}{t-(t'-t'')}\right).$$

For values of $t' \gg t_0$ this expression further simplifies to

$$n_{2L} = \frac{-Q_0 t_0}{t^3} e^{-\omega_a t} \Phi_s\left(\frac{\mathbf{x}}{t}\right) \int_0^t dt' \omega\left(\frac{\mathbf{x}t'}{t}, t'\right). \tag{25}$$

Now consider the gain term n_{2G} in (23):

$$n_{2G} = \int_0^t dt' \int d^3y \frac{e^{-\omega_a(t-t')}}{(t-t')^3} \omega n \Phi\left(y, \frac{\mathbf{x}-\mathbf{y}}{t-t'}, t'\right). \tag{26}$$

For times t' much greater than t_0, equation (21) may be used in (26). The expression for Φ then becomes

$$\left[\frac{18}{\pi}\left(\frac{t'}{y}\right)^2\left(\frac{t'}{t_0}\right)^2\right]^{\frac{3}{2}} \exp\left\{-18\left(\frac{t}{t_0}\right)^2\left(\frac{t'}{t-t'}\right)^2\frac{1}{y^2}\left[\mathbf{y}-\mathbf{x}\frac{t'}{t}\right]^2\right\}.$$

Since $18(t/t_0)^2 \gg 1$, application of the saddle-point method to (26) yields the result

$$n_{2G} = \int_0^t dt'\, e^{-\omega_a(t-t')}\left(\frac{t'}{t}\right)^3 \omega\left(\frac{\mathbf{x}t'}{t}, t'\right) n\left(\frac{\mathbf{x}t'}{t}, t'\right).$$

But $n(\mathbf{x}t'/t, t')$ is given by (21) as

$$\frac{Q_0 t_0}{t'^3} e^{-\omega_a t'} \Phi_s\left(\frac{\mathbf{x}}{t}\right).$$

Thus, to the present order of approximation

$$n_{2G} = \frac{Q_0 t_0}{t^3} e^{-\omega_a t} \Phi_s\left(\frac{\mathbf{x}}{t}\right) \int_0^t dt' \omega\left(\frac{\mathbf{x}t'}{t}\right) = -n_L.$$

The approximate cancellation is clearly due to the rapid decay of the translational temperature as the gas expands away from the continuum region after the engine shut sdown. Since the above calculation neglects terms of $O(t_0/t)$ compared with unity, the relative size estimate is more accurately given as

$$\frac{n_2}{n_1} \sim O\left(\frac{t_0}{t}\int_0^t dt' \omega\left(\frac{\mathbf{x}t'}{t}, t'\right)\right).$$

It is now easy to show that $n_2/n_1 \ll 1$. The self-collision frequency ω may be represented in the form $\omega = c_s \sigma n_1(\mathbf{x}, t)$ and σ is the effective mean collision cross-section. Here c_s is the thermal speed $(2kT_s/m)^{\frac{1}{2}}$. Taking the thermal speed to be constant is the most conservative case and corresponds to a Maxwell molecule interaction potential. If the exponential terms in the representation (21) for n_1 are assumed all to be unity, the ratio n_2/n_1 becomes

$$n_2/n_1 \sim t_0 c_s \sigma Q_0 t_0 / c_s^3 t^3.$$

Let the time t be of $O(\omega_a^{-1})$, the scale on which the interaction with the ambient atmosphere occurs. Then if the ambient and self-collision cross-sections are assumed similar in size, this expression can be rewritten as

$$\frac{n_2}{n_1} \sim \frac{u_s t_0}{\lambda_a} \frac{1}{W_s}\left(\frac{T_a}{T_s}\right)^{\frac{3}{2}}\left(\frac{Q_0 t_0}{n_a \lambda_a^3}\right). \tag{27}$$

Note that the smallness of the last factor in (27) is a basic assumption for the entire analysis. Moreover, the ratio $u_s t_0/\lambda_a$ (the fraction of a mean free path that a molecule moving with the source velocity would travel while the motor is operating) is also small. The assumption that $n_2/n_1 \ll 1$ invoked at the outset is then certainly justified. The self-scattering contribution may thus be ignored in calculating the far-field interaction of the exhaust gas with the atmosphere, and will not be considered further in this work.

6. The scattering Green's function

At this stage, the only role played by the ambient atmosphere is the exponential attenuation of the free molecular flow described in the previous sections. The cloud of scattered particles $n_3(\mathbf{x}, t)$ is represented in (11*b*) by a convolution of the free molecular flow with the scattering Green's function. The Green's function $G(\mathbf{x}, t)$ will be studied in this section, while the composite flow pattern will be discussed in the following section.

The starting-point for the analysis is the transform representation of G in (11*c*). The velocity integration in that expression may be readily carried out to yield

$$G(\mathbf{x}^*, t^*) = \frac{1}{2\pi i}\frac{1}{(2\pi)^3}\int dp \int d^3k\, e^{i\mathbf{k}.\mathbf{x}^* + pt^*}\frac{\pi^{\frac{1}{2}}}{k}\frac{w(Z_a)}{1-\pi^{\frac{1}{2}}k^{-1}w(Z_a)}, \tag{28a}$$

$$w(Z_a) = \frac{i}{\pi}\int_{-\infty}^{\infty}\frac{e^{-t^2}dt}{Z_a - t}, \quad Z_a = \left(i\frac{p+1}{k} - \frac{\mathbf{a}.\mathbf{k}}{k}W_a\right), \tag{28b}$$

$$W_a = \frac{u_a}{(2kT_a/m)^{\frac{1}{2}}} \quad \mathbf{x}^* = \frac{\mathbf{x}}{\lambda_a}, \quad t^* = \omega_a t. \tag{28c}$$

The spatial co-ordinates $\mathbf{x}^*$ have been non-dimensionalized with respect to the ambient mean free path λ_a, while the natural time scale t^* is measured in mean collision times ω_a^{-1}. The function $w(Z_a)$ is described in detail by Abramowitz & Stegun (1965), where all properties needed in what follows may be found.

First consider the inversion over the Laplace transform variable p. Since the inversion contour integral c is defined (figure 2) for $\mathrm{Re}\,(p) > 0$ and $\mathbf{k}$ is real, $\mathrm{Im}\,(Z_a) > 0$. Under these conditions $w(Z_a)$ is an analytic function which is real only for imaginary Z_a. Thus the only singularity in the integrand of G in the right half p plane is a pole at

$$k = \pi^{\frac{1}{2}}w(i\lambda), \quad p + 1 + i(\mathbf{a}.\mathbf{k})\,W_a = k\lambda, \quad w(i\lambda) = e^{\lambda^2}\operatorname{erfc}\lambda. \tag{29}$$

The contour is now moved to the left of the pole whose location is given by (29). The residue at the pole is

$$\frac{1}{2(2\pi)^3}\int d^3k\, e^{i\mathbf{k}.[\mathbf{x}^* - \mathbf{a}W_a t^*]}\frac{k^2 H(\pi^{\frac{1}{2}} - k)}{1 - k\lambda(k)}\,.\,e^{-\{1-k\lambda(k)\}t^*}. \tag{30}$$

Here H is the unit step function and $\lambda(k)$ is the inverse of the function defined in (28). The Fourier inversion in (30) may now be reduced by noting that the only

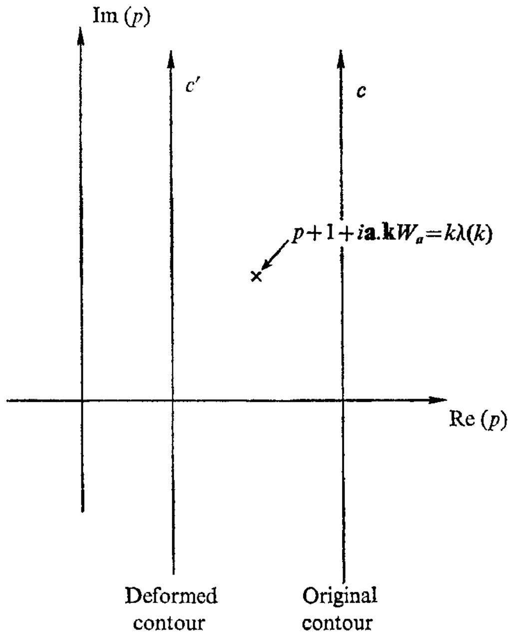

FIGURE 2. Laplace transform inversion contours used to obtain (31).

vector in the integrand is $\mathbf{x}^* - \mathbf{a}W_a t^*$. Defining a spherical polar co-ordinate system in $\mathbf{k}$ space with $\mathbf{x}^* - \mathbf{a}W_a t$ as the pole, the angular integrals are easily evaluated, leaving

$$\frac{1}{(2\pi)^2} e^{-t^*} \int_0^{\pi^{\frac{1}{2}}} dk \frac{k^4}{1-k\lambda(k)} \frac{\sin kr^*}{kr^*} e^{k\lambda(k)t^*}, \tag{31}$$

$$r^* = |\mathbf{x} - \mathbf{a}W_a t^*|.$$

Inspection of the remaining contour integral c' (see figure 2) shows that G is a function only of the two variables r^* and t^*. To take advantage of this fact, p is replaced with the complex variable ρ defined by

$$p + 1 + i(\mathbf{a}.\mathbf{k}) W_a = -ik\rho.$$

Again k is real so $\mathrm{Im}\,\rho > 0$ on c'. Now multiply the integrand by a convergence factor $e^{-\epsilon k}$, where $\epsilon > 0$. Eventually ϵ will be put equal to zero. The contour c' can now be shifted to the real axis in the ρ plane, and the $\mathbf{k}$ integrations reduced as before to obtain

$$G(r^*, t^*) = \frac{1}{(2\pi)^2} \int_0^{\pi^{\frac{1}{2}}} dk\, k^4 \frac{e^{-[1-k\lambda(k)]t^*}}{1-k\lambda(k)} \frac{\sin kr^*}{kr^*}$$

$$+ \frac{e^{-t^*}}{4\pi^3} \int_0^\infty dk\, k^3 \frac{\sin kr^*}{kr^*} e^{-\epsilon k} \int_{-\infty}^{\infty} d\rho \frac{\pi^{\frac{1}{2}}}{k} \frac{w_+(\rho)\, e^{-ik\rho t}}{1 - \pi^{\frac{1}{2}} k^{-1} w_+(\rho)}, \tag{32}$$

$$w_+(\rho) = e^{-\rho^2} + i \frac{2}{\pi^{\frac{1}{2}}} e^{-\rho^2} \int_0^\rho e^{t^2}\, dt.$$

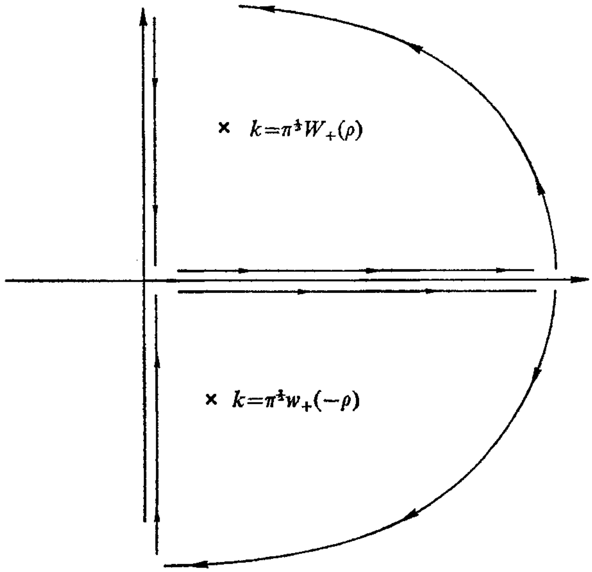

FIGURE 3. Contour integration used to evaluate $I(\rho)$ in (33).

The variable ρ is now real. To proceed further with the second expression in (32) it is convenient to interchange orders of integration holding ρ fixed and real and consider the inner integral $K(\rho)$:

$$K \equiv \int_0^\infty dk\, k^2 \frac{\sin kr^*}{kr^*} \frac{e^{-\epsilon k - ik\rho t^*}}{1-\pi^{\frac{1}{2}}k^{-1}w_+(\rho)}$$

$$= \frac{1}{2ir^*}\{I(r^*-\rho t^*) - I[-r(r^*+\rho t^*)]\},$$

where

$$I(\zeta) = \int_0^\infty dk\, k^2 \frac{e^{ik\zeta-\epsilon k}}{k-\pi^{\frac{1}{2}}w_+(\rho)} \tag{33}$$

For $\zeta > 0$ equation (33) may be evaluated by considering the integral over the upper contour shown in figure 3. For $\zeta > 0$ the lower contour in figure 3 may be used. The result is

$$I(\zeta) = \frac{2i\rho}{|\rho|}[\pi w_+(\rho)]^2 e^{\alpha} H(\rho\zeta) + [\pi^{\frac{1}{2}}w_+(\rho)]^2\left\{\frac{1}{\alpha^2}-\frac{1}{\alpha}+e^{\alpha}E_1(\alpha)\right\}, \tag{34}$$

$$\alpha = (\zeta+i\epsilon)\, i\pi^{\frac{1}{2}}w_+(\rho).$$

The function $E_1(\alpha)$ in (34) is the exponential integral $E_1(\alpha)$ defined by

$$E_1(\alpha) = \int_\alpha^\infty e^{-t}\frac{dt}{t}.$$

The second expression in (32) now becomes

$$\frac{e^{-t^*}}{4\pi^{\frac{5}{2}}}\int_{-\infty}^{\infty} d\rho\, \frac{w_+(\rho)}{2ir^*}\{I(r^*-\rho t^*) - I[-(r^*+\rho t^*)]\}. \tag{35}$$

Equation (35) may be evaluated as a sum of four terms. First, the terms proportional to α^{-2} in $I(\rho)$ make a contribution

$$\frac{i\,e^{-t^*}}{8\pi^{\frac{5}{2}}r^*}\int_{-\infty}^{\infty} w_+(\rho)\, d\rho\left\{\left[\frac{1}{r^*-\rho t^*+i\epsilon}\right]^2 - \left[\frac{1}{r^*+\rho t^*-i\epsilon}\right]^2\right\}.$$

Using the fact that $w_+(\rho)$ is analytic in the upper half-plane and has the asymptotic behaviour

$$w_+(\rho) \sim i/\pi^{\frac{1}{2}}\rho, \quad \rho \to \infty, \tag{36}$$

the contribution of the α^{-2} terms is

$$\frac{-e^{-t^*}}{4\pi^{\frac{3}{2}} r^* t^{*2}} \left[w'_+ \left(\frac{r^*}{t^*}\right) - w'_+ \left(-\frac{r^*}{t^*}\right) \right] = \frac{1}{(\pi^{\frac{1}{2}} t^*)^3} \exp\left[-t^* - (r^*/t^*)^2\right].$$

Here, the limit $\epsilon \to 0$ has been taken after performing the integration. Using identical analysis on the α^{-1} contribution to (35) gives the result

$$\frac{2\,e^{-t^*-2\xi^2}}{\pi^{\frac{3}{2}} t^{*2}} \frac{1}{\xi} \int_0^{\xi} e^{x^2}\, dx \quad \left(\xi = \frac{r^*}{t^*}\right).$$

The term proportional to $e^{\alpha} H(\rho\zeta)$ in $I(\zeta)$ leads to the following expression:

$$\frac{e^{-t^*}}{4\pi^{\frac{1}{2}} t^*} \frac{1}{\xi} \int_0^{\xi} d\rho \exp\left[-v\pi^{\frac{1}{2}} t^* (\xi - \rho)\right] \{2u(u^2 - 3v^2)$$
$$\times \cos\left[\pi^{\frac{1}{2}} u t^* (\xi - \rho)\right] - 2v(3u^2 - v^2) \sin\left[\pi^{\frac{1}{2}} u t^* (\xi - \rho)\right]\},$$
$$v(\rho) = \frac{2}{\pi^{\frac{1}{2}}} e^{-\rho^2} \int_0^{\rho} e^{t^2}\, dt, \quad u(\rho) = e^{-\rho^2}.$$

The remaining contribution is

$$\frac{e^{-t^*}}{i(2\pi^{\frac{1}{2}})^3 t^*} \frac{1}{\xi} \int_{-\infty}^{\infty} d\rho\, [w_+(\rho)]^3 \{\exp\left[i\pi^{\frac{1}{2}} t^* (\xi - \rho)\, w_+(\rho)\right] E_1\left[i\pi^{\frac{1}{2}} t^* (\xi - \rho)\, w_+(\rho)\right]$$
$$- \exp\left[-i\pi^{\frac{1}{2}} t^* (\xi + \rho)\, w_+(\rho)\right] E_1\left[-i\pi^{\frac{1}{2}} (r^* + \rho t^*)\, w_+(\rho)\right]\}.$$

Collecting all terms, the Green's function is given exactly by

$$G(r^*, t^*) = \frac{1}{(2\pi)^2} \int_0^{\pi^{\frac{1}{2}}} dk\, k^4 \frac{e^{-[1 - k\lambda(k)]t^*}}{[1 - k\lambda(k)]} \frac{\sin kr^*}{kr^*}$$
$$+ \frac{e^{-t^*}}{\pi^{\frac{3}{2}}} \left\{ \frac{e^{-\xi^2}}{t^{*3}} + \frac{2}{t^{*2}} e^{-2\xi^2} \frac{1}{\xi} \int_0^{\xi} e^{x^2}\, dx + \frac{\pi}{4t^* \xi} \int_0^{\xi} d\rho \exp\left[-v\pi^{\frac{1}{2}} t^* (\xi - \rho)\right] \right.$$
$$\times \left\{ 2u(u^2 - 3v^2) \cos\left[\pi^{\frac{1}{2}} u t^* (\xi - \rho)\right] - 2v(3u^2 - v^2) \sin\left[\pi^{\frac{1}{2}} u t^* (\xi - \rho)\right] \right\}$$
$$\left. + \frac{1}{8it^*} \frac{1}{\xi} \int_{-\infty}^{\infty} d\rho\, [w_+(\rho)]^3 \{ e^{Z_1} E_1(Z_1) - e^{Z_2} E_1(Z_2) \} \right\}, \tag{37}$$
$$Z_1 = i\pi^{\frac{1}{2}} t^* (\xi - \rho)\, w_+(\rho), \quad Z_2 = -i\pi^{\frac{1}{2}} t^* (\xi + \rho)\, w_+(\rho),$$
$$w_+(\rho) = u(\rho) + iv(\rho), \quad \xi = r^*/t^*, \quad k = \pi^{\frac{1}{2}} e^{\lambda^2} \operatorname{erfc} \lambda.$$

This expression cannot be reduced further by analytical methods for arbitrary values of r^* and t^*. However, the result (37) simplifies greatly for two important limiting cases. First, when t^* is small and ξ is fixed the early-time approximation to G is easily seen from (37) to be

$$G(r^*, t^*) \simeq \frac{e^{-\xi^2}}{(\pi^{\frac{1}{2}} t^*)^3} \left\{ 1 + t^* \left[\frac{2e^{-\xi^2}}{\xi} \int_0^{\xi} e^{x^2}\, dx - 1 \right] + O(t^{*2}) \right\}. \tag{38}$$

Thus for early times G has a distinctly free molecular behaviour. For large t^* and $r^*(t^*)^{-\frac{1}{2}}$ fixed all terms except the first in (37) are exponentially small.

The long-time behaviour is evidently contained in the first integral. Since r^* is also large, a non-trivial result can only come from small k. However, small k corresponds to large λ:

$$k \cong \frac{1}{\lambda}\left\{1-\frac{2}{\lambda^2}+\ldots\right\}.$$

The major contribution comes from small k permitting the integral to be extended to infinity with negligible error. Thus

$$G(r^*,t^*) \cong \frac{1}{2(\pi)^2}\int_0^\infty dk\, k^2 \exp\left[-\tfrac{1}{2}k^2t^*\right]\frac{\sin kr^*}{kr^*}$$
$$= \frac{\exp(-r^{*2}/2t^*)}{(2\pi t^*)^{\frac{3}{2}}}. \qquad (39)$$

This is the familiar diffusion Gaussian Green's function. Remembering that r^* is given in terms of $\mathbf{x}^*$ and t^* by

$$r^* = |\mathbf{x}^* - \mathbf{a}W_a t^*|$$

it is clear that the interaction evolves from a nearly collisionless phenomenon to a collision-dominated diffusion in a uniform flow.

The asymptotic limiting forms of G given by (38) and (39) both have the important property

$$\int G(\mathbf{x},t)\, d^3x = 1. \qquad (40)$$

Applying the relation

$$\int d^3x G(\mathbf{x},t) = \lim_{k\to 0}\frac{1}{2\pi i}\int dp\, e^{pt}\, G(\mathbf{k},p)$$

to (28) and employing (36); it is easy to see that (40) holds exactly for all times.

The expression (37) for $G(r^*,t^*)$ has been programmed for use on a Univac 1108 computer. The intervals were evaluated using up to 32 points in the Gaussian quadrature method. The estimated error is about 0·2 % for values of r^* such that

$$G(r^*,t^*)/G(0,t^*) \geqslant 10^{-3}.$$

The results for G are plotted versus r^* for selected values of t^* between 0·1 and 10·0 in figures 4(*a*)–(*d*). Figure 5 displays $G(0,t^*)$. The final asymptotic form given by (39) is actually approached quite slowly. Approximately thirty mean collision times are required to obtain better than 10% accuracy using this expression, and the error is still about 5 % at fifty mean collision times. The computing time was approximately 0·5 s for each value of (r^*,t^*). This results in prohibitively long (and expensive) calculations for the composite flow field n_1+n_3. To reduce the computing time, the accuracy requirements for the determination of G were relaxed. Inspection of the results showed that the last integral in (37) is approximately 0·01 G in the r^*, t^* domain investigated. Elimination of this term and corresponding reductions in accuracy in the remaining quadrature routines reduced the computing time per point to 0·05 s with an estimated 2 % error in G. The reduced program was used to obtain the results shown in the following section.

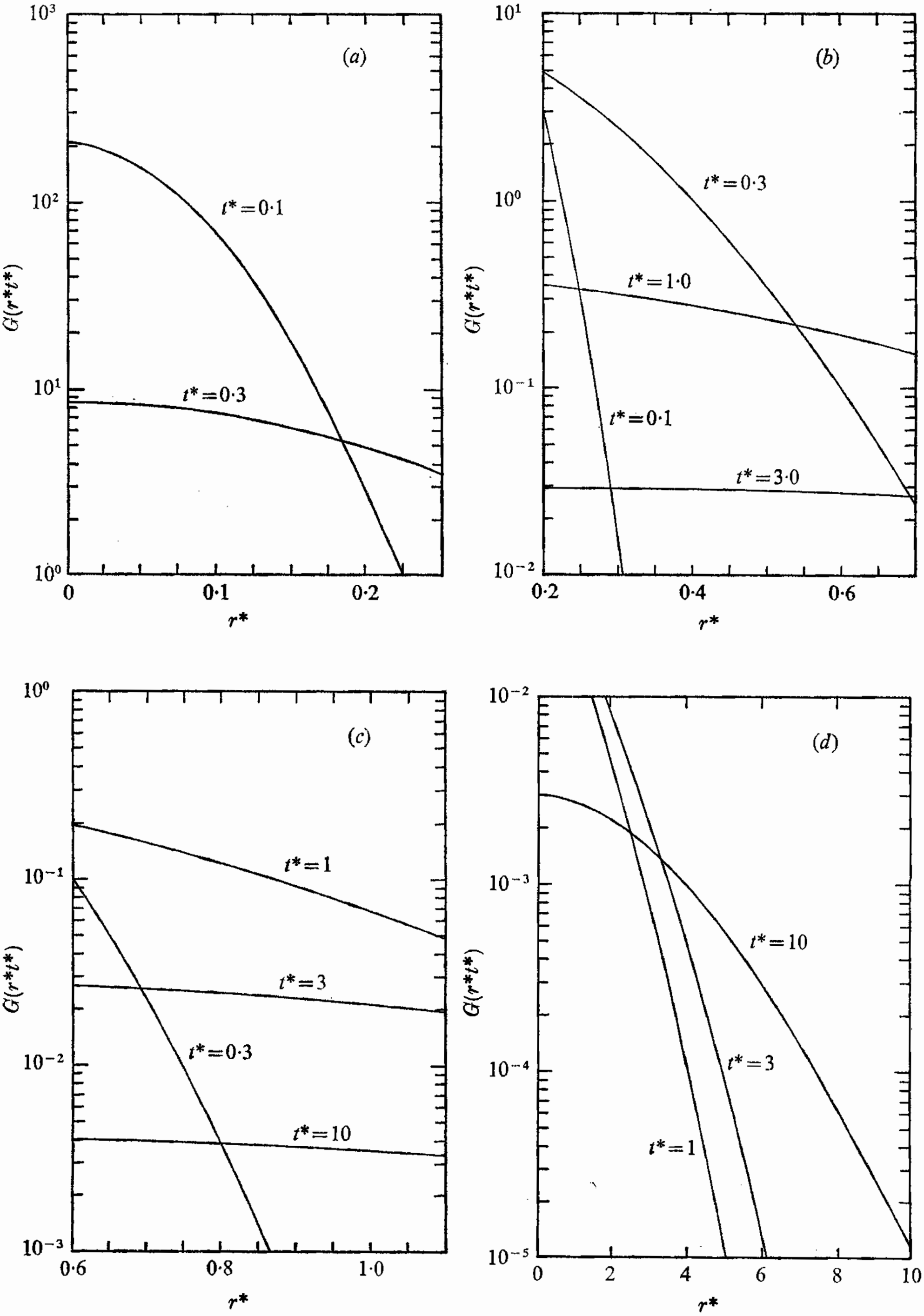

FIGURE 4. Evolution of the scattering Green's function at (a) early times, $0 \leqslant r^* \leqslant 0{\cdot}25$; (b) intermediate times, $0{\cdot}2 \leqslant r^* \leqslant 0{\cdot}7$; (c) intermediate times, $0{\cdot}6 \leqslant r^* \leqslant 1{\cdot}1$; (d) long times, $0 \leqslant r^* \leqslant 10{\cdot}0$.

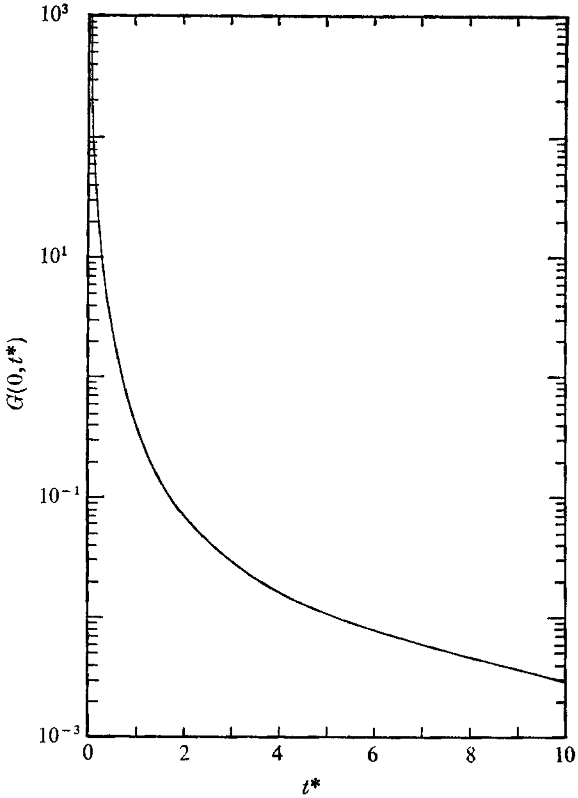

FIGURE 5. Decay of the maximum value of the scattering Green's function $G(0, t^*)$.

7. The composite flow

The cloud of scattered molecules $n_3(\mathbf{x}, t)$ may be represented in the form

$$n_3 = \int_0^{t^*} dt' \int d^3x' n_1(\mathbf{x}', t')\, G(\mathbf{x}^* - \mathbf{x}', t^* - t'), \tag{41}$$

$$n_1(\mathbf{x}^*, t') = Q_0 \omega_a^2 \frac{m^{\frac{3}{2}}}{2\pi k T s} \int_{t^* - \omega_a t_0}^{t^*} dt J(t),$$

$$J(t) = \frac{1}{t^3} \exp\left\{-t - \left[\left(\frac{T_a}{T_s}\right)^{\frac{1}{2}} \frac{\mathbf{x}}{t} - W_s \mathbf{s}\right]^2\right\}.$$

This expression, together with equation (15) for n_1 and the results of the previous section, constitutes the complete description of the exhaust gas density. However, while (15) is directly usable for numerical computation, (41) is not. The chief obstacle to the use of (41) is the prohibitive time and expense associated with the spatial integrations. An approximate evaluation of these integrals is necessary to obtain flow field results.

Consider (41) for times sufficiently large for the asymptotic result (39) to apply. Under these conditions (41) becomes

$$n_3 = Q_0 \omega_a^2 \left(\frac{m}{2\pi k T s}\right)^{\frac{3}{2}} \int_0^{t^*} dr' \int_{t' - \omega_a t_0}^{t'} dt\, t^{-3} e^{-t} \left[2\pi (t^* - t')\right]^{\frac{3}{2}} K, \tag{42}$$

$$K = \int d^3x' \exp\left\{-\left[\left(\frac{T_a}{T_s}\right)^{\frac{1}{2}}\frac{\mathbf{x}'}{t} - W_s\mathbf{s}\right]^2 - [\mathbf{x}^* - \mathbf{x}' - \mathbf{a}W_a(t^*-t')]^2/2(t^*-t')\right\}.$$

The evaluation of K is straightforward, yielding the result

$$n_3 \cong Q_0 t_0 \omega_a^3 \left(\frac{m}{2kT_a}\right)^{\frac{3}{2}} \int_0^{t^*} dt' \left\{\pi\left[2(t^*-t') + \frac{T_s}{T_a}t'^2\right]\right\}^{-\frac{3}{2}}$$
$$\times \exp\left\{-t' - \left[2(t^*-t') + \frac{T_s}{T_a}t'^2\right]^{-1}\left[\mathbf{x}^* - \mathbf{a}W_a(t^*-t') - W_s\left(\frac{T_s}{T_a}\right)^{\frac{1}{2}}t'\mathbf{s}\right]^2\right\}. \quad (43)$$

The assumption $\omega_a t_0 \ll t$ has also been employed to obtain (43). Comparison of this expression with (39) enables (43) to be written in the more revealing form

$$n_3 \cong Q_0 t_0 \omega_a^3 \left(\frac{m}{2kT_a}\right)^{\frac{3}{2}} \int_0^{t^*} dt'\, e^{-t'} G(r,\tau), \quad (44)$$
$$r = |\mathbf{x}^* - \mathbf{a}W_a(t^*-t') - W_s(T_a/T_s)^{\frac{1}{2}}t'\mathbf{s}|,$$
$$\tau = t^* - t' + \tfrac{1}{2}(T_s/T_a)t'^2.$$

The result (44) is actually valid under a much wider range of conditions than those implied by the above derivation. For times $t^* \ll 1$, substitution of the leading term in (38) into (41) again yields (44). Moreover, for W_s large and $W_s(T_s/T_a)^{\frac{1}{2}}t^*$ fixed, a similar result can be obtained as follows.

Consider the integral over $\mathbf{x}'$ in (41). Since G is a function of r^* and t^* only, this expression can be written as

$$\int d^3x' J(t)\, G(|\mathbf{x}^* - \mathbf{x}' - \mathbf{a}W_a(t^*-t')|, t^*-t').$$

Under the stated conditions, application of the saddle-point method to the above integral leads to the result

$$n_3 \cong Q_0 t_0 \omega_a^3 \left(\frac{m}{2kT_a}\right)^{\frac{3}{2}} \int_0^{t^*} dt'\, e^{-t'} G(r, t^*-t'). \quad (45)$$

Equation (45) differs from (44) only in the dependence of the variable τ on t'. For $W_s(T_s/T_a)^{\frac{1}{2}}t^*$ fixed and $W_s \gg 1$, the term $\frac{1}{2}(T_s/T_a)t'^2$ in the expression (44) for τ is $O(W_s^{-2})$. For times t^* such that this contribution to τ is of $O(1)$, τ is of $O(W_s^2)$ and (44) holds.

The final formulae for the exhaust gas density distribution have been programmed in the following form:

$$\frac{n\lambda_a^3}{Q_0 t_0} = N_1 e^{-t^*} + \int_0^{t^*} dt\, e^{-t} G(r,\tau), \quad (46)$$
$$N_1 = \frac{\exp\{-W_s^2 \sin^2\theta\}}{\pi^{\frac{3}{2}}\omega_a t_0 (x^*)^2}\left(\frac{T_a}{T_s}\right)^{\frac{1}{2}}[F_1(\beta) - F_1(\alpha)],$$
$$\alpha = \left(\frac{T_a}{T_s}\right)^{\frac{1}{2}}\frac{x^*}{t^*} - W_s\cos\theta, \quad \beta - \alpha = \left(\frac{T_a}{T_s}\right)^{\frac{1}{2}}\frac{x^*}{t^*}\left(\frac{\omega_a t_0}{t^* - \omega_a t_0}\right).$$

The function F_1 is defined in (15b), while the computation of G is explained in the preceding section.

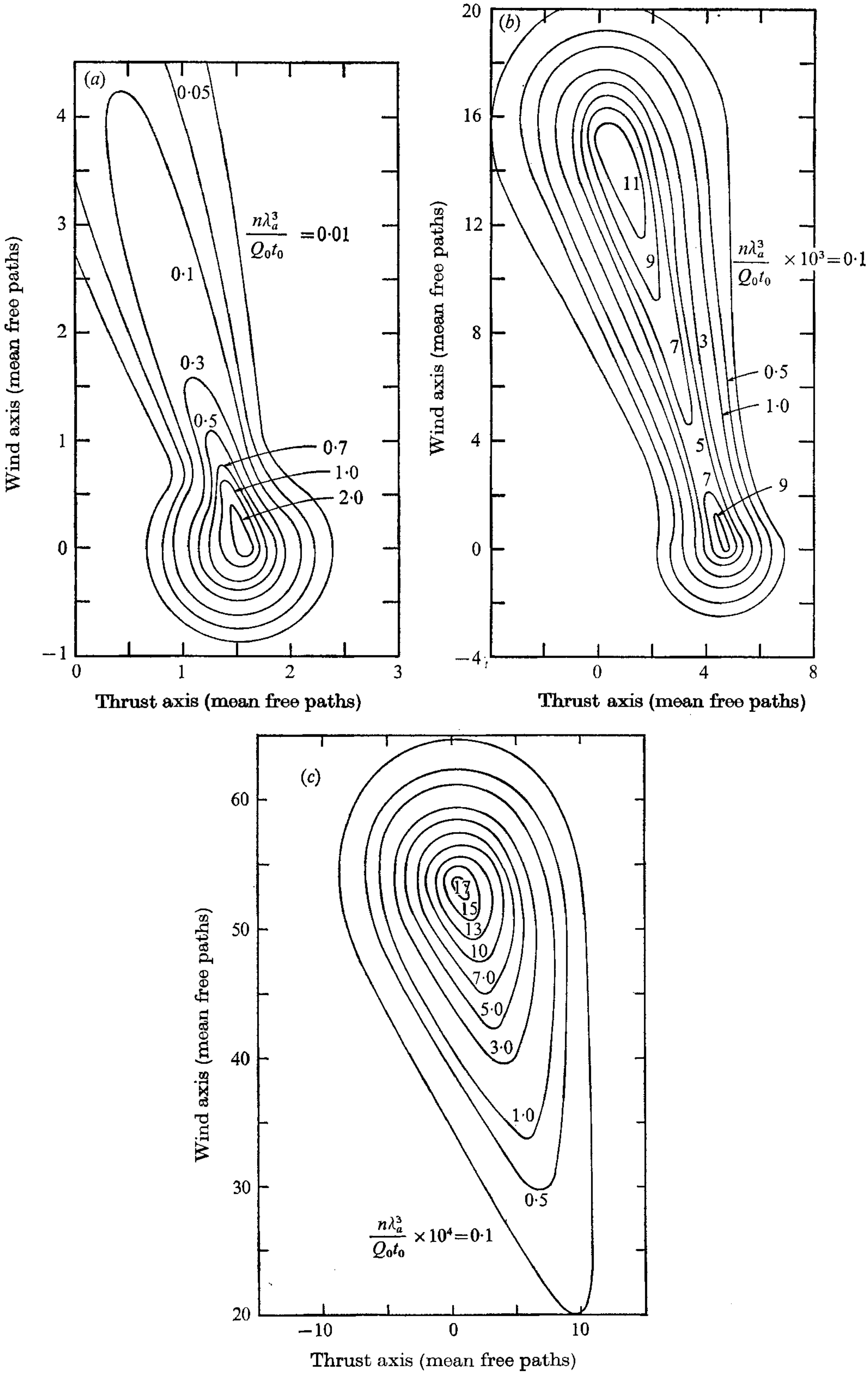

FIGURE 6. Isopycnal contours of $n\lambda_a^3\,(Q_0 t_0)^{-1}$ at (*a*) $t^* = 1$, (*b*) $t^* = 3$ and (*c*) $t^* = 10$ in the plane $\phi = 0$. $M_e = 4{\cdot}77$, $\gamma = 1{\cdot}266$, $\omega_a t_0 = 0{\cdot}102$, $W_a = 5{\cdot}60$, $\psi = 90°$, $T_e/T_a = 0{\cdot}166$.

As an example, the exhaust plume of a motor operating at right angles to the ambient wind is presented in figures 6 (*a*)–(*c*). The isopycnal contours in the plane containing the thrust vector and the wind vector are plotted at one, three and ten mean collision times respectively. The values of the six parameters M_e, $\gamma, \omega_a t_0, W_a, T_e/T_a$ and ψ necessary to specify the flow uniquely are given in the caption.

The nearly circular portion of the isopycnal contours at one collision time is due to the free molecular flow. The isopycnal contours of this flow are nearly spherically symmetric about the point $\mathbf{x}^* = (T_s/T_a)^{\frac{1}{2}} W_s \mathbf{s} t^*$ for $t^* \gg \omega_a t_0$. The long tongue of gas pointing toward the wind axis represents the cloud of scattered molecules caught up in the ambient wind. At three collision times the bimodal nature of the distribution is most evident. The scattered gas cloud and the free molecular flow have almost the same peak density. Note that the absolute level of the free molecular number density has fallen by two orders of magnitude in the interval. At ten collision times the flow is dominated by the scattered gas cloud. The tail is caused by the weighted effect of collisions at times $t' < t^*$ on the density (see the integral in (44)). Ultimately, the tail disappears and the flow asymptotically becomes spherically symmetric about $\mathbf{x}^* = \mathbf{a} W_a t^*$ with the density given by

$$\frac{n\lambda_a^3}{Q_0 t_0} \simeq \frac{1}{(2\pi t^*)^{\frac{3}{2}}} \exp\left\{-\frac{[x^* - aW_a t^*]^2}{2t^*}\right\}.$$

The author is grateful to Dr Kevin S. Tait and Dr Apostoles E. Germeles for performing the numerical computations reported here. This work was supported by the Army Ballistic Missile Defense Agency under Contract Number DAHC60-71-C-0084.

REFERENCES

ABRAMOWITZ, M. & STEGUN, I. A. 1966 *Handbook of Mathematical Functions*. U.S. Government Printing Office.

BROOK, J. W. & HAMEL, B. B. 1972 Spherical source flow with a finite back pressure. *Phys. Fluids*, **15**, 1898.

BROOK, J. W. & OMAN, R. A. 1965 Steady expansions at high speed ratio using the BGK kinetic model. In *Rarefied Gas Dynamics – Fourth Symposium* (ed. J. H. deLeeuw), p. 125.

CHEN, T. Y. 1970 Finite source Reynolds number effects on temperature freezing in a spherically symmetric expansion. *Phys. Fluids*, **13**, 317.

DRAPER, J. S. & HILL, J. A. F. 1969 Rarefaction in underexpanded flows. *A.I.A.A. J.* **7**, 1400.

EDWARDS, R. N. & CHENG, H. K. 1966 Steady expansion of a gas into a vacuum. *A.I.A.A. J.* **4**, 558.

FREEMAN, N. C. & GRUNDY, R. E. 1968 Solutions of the Boltzmann equation in an unsteady cylindrically symmetric expansion. *J. Fluid Mech.* **31**, 723.

GROSS, E P. & KROOK, M. 1956 Model for collision processes in gases: small-amplitude oscillations of charged two-component systems. *Phys. Rev.* **102**, 593.

GRUNDY, R. E. 1969 Axially symmetric expansion of a monatomic gas from an orifice into a vacuum. *Phys. Fluids*, **12**, 2011.

GRUNDY, R. E. & THOMAS, D. R. 1969 The unsteady spherically symmetric of a fixed mass of gas into a vacuum *A.I.A.A. J.* **7**, 967.

HAMEL, B. B. & WILLIS, D. R. 1966 Kinetic theory of source flow expansion with application to the free jet. *Phys. Fluids*, **9**, 829.

PERACCHIO, A. A. 1970 Kinetic theory analysis for the flowfield of a two-dimensional nozzle exhausting to vacuum. *A.I.A.A. J.* **8**, 1965.

THOMAS, D. R. 1971 Spherical expansion into vacuum: a higher-order analysis *A.I.A.A. J.* **9**, 451.